Heterozygous *Cc2d1a* mice show sex-dependent changes in the Beclin-1/p62 ratio with impaired prefrontal cortex and hippocampal autophagy

Elif Funda Sener [a,b,*], Halime Dana [a,b], Reyhan Tahtasakal [a,b], Zuhal Hamurcu [a,b], Serpil Taheri [a,b], Nesrin Delibasi [c], Ecmel Mehmetbeyoglu [b,d], Zeynep Yilmaz Sukranli [b], Fatma Dal [b], Esra Tufan [b], Asli Okan Oflamaz [e], Zuleyha Doganyigit [e], Yusuf Ozkul [b,f], Minoo Rassoulzadegan [b,g]

[a] *Erciyes University Medical Faculty Department of Medical Biology, 38039, Kayseri-Turkey*
[b] *Erciyes University Genome and Stem Cell Center (GENKOK), 38039, Kayseri-Turkey*
[c] *Cappodoccia University, Cappadocia Vocational School Medical Laboratory Techniques Programme, Nevsehir-Turkey*
[d] *Cardiff University School of Medicine Department of Hematology, Division of Cancer and Genetics, Cardiff-UK*
[e] *Bozok University Medical Faculty Department of Histology and Embryology, 66100, Yozgat-Turkey*
[f] *Erciyes University Medical Faculty Department of Medical Genetics, 38039, Kayseri-Turkey*
[g] *Université Cote d'Azur (UCA), INSERM-CNRS, IRCAN, 06107 Nice, France*

ARTICLE INFO

ABSTRACT

Autism Spectrum Disorders (ASD) are a group of neurodevelopmental disorders characterized by repetitive behaviors, lack of social interaction and communication. *CC2D1A* is identified in patients as an autism risk gene. Recently, we suggested that heterozygous *Cc2d1a* mice exhibit impaired autophagy in the hippocampus. We now report the analysis of autophagy markers (Lc3, Beclin and p62) in different regions hippocampus, prefrontal cortex, hypothalamus and cerebellum, with an overall decrease in autophagy and changes in Beclin-1/p62 ratio in the hippocampus. We observed sex-dependent variations in transcripts and protein expression levels. Moreover, our analyses suggest that alterations in autophagy initiated in *Cc2d1a* heterozygous parents are variably transmitted to offspring, even when the offspring's genotype is wild type. Aberration in the autophagy mechanism may indirectly contribute to induce synapse alteration in the ASD brain.

1. Introduction

Autism spectrum disorder (ASD) is a neurodevelopmental disorder detected in early childhood (Baribeau and Anagnostou, 2022; Ozkul et al., 2020). Current DSM-5 suggests two main diagnostic criteria of ASD: i) a child must have persistent deficits in each of three areas of social communication and interaction and ii) at least two of four types of restricted, repetitive behaviors. The specific pathogenic mechanisms of ASDs are poorly understood (Wu et al., 2020). The phenotype and severity of ASD, are extremely heterogeneous (Baribeau and Anagnostou, 2022; Calderoni, 2022). Patients with ASD show significant

genetic, transcription levels, behavioral, etiological, and pathophysiological heterogeneity (Citrigno et al., 2020). Several factors contribute to the heterogeneity of ASD, with high rates of psychiatric disorders (such as attention deficit hyperactivity and anxiety), neurological disorders (such as seizures, sensory and motor), and comorbid medical conditions (e.g., sleep, gastrointestinal, immune system disorders) (Dana et al., 2020a). There are currently no pharmacologic agents to treat the main symptoms of ASD. Many psychopharmacologic agents with new molecular mechanisms and/or new targets, show promise in most early-stage trials (Baribeau and Anagnostou, 2022).

The Coiled-coil and C2 domain containing 1A (*CC2D1A*) is a

conserved protein, and identified mutations in the human *CC2D1A* gene lead to nonsyndromic autosomal recessive intellectual disability and are classified as an autism risk gene (Basel-Vanagaite et al., 2006; Sener et al., 2016; Sener et al., 2020). CC2D1A is a transcriptional repressor; there is evidence for its role in several cell signaling pathways, including nuclear factor-κB (NF-κB) and protein kinase B (PKB). *Cc2d1a* transcripts (mouse homologue) are abundantly detected in the brain (especially in the cerebral cortex, hippocampus, basal ganglia, and hypothalamus), but little information is known about its physiological function (Yang et al., 2019). While the molecular properties of *CC2D1A* have been elucidated in recent years, most functional studies have been performed in cell culture systems. The functional relevance of *Cc2d1a* in vivo with knock-in transgenic mouse models has just begun to be characterized (Dana et al., 2020a; Basel-Vanagaite et al., 2006; Sener et al., 2016; Sener et al., 2020; Yang et al., 2019; Wang et al., 2023). Assessing autism-relevant behavioral changes in mice is challenging, but the possibility of functional testing with homogeneous underlying genetic control in mice allows the study of mechanisms involved in behavioral alteration.

Macroautophagy (referred to here as autophagy) is a process of degradation of long-lived proteins and damaged organelles (Lieberman et al., 2020). Autophagy functions as both a survival and cell death mechanism. Neuronal autophagy is very important in the interplay between neurons, signaling and development, and impaired autophagy negatively affects neuron growth and functions (Lee et al., 2013). Neuronal autophagy plays a key role in protein balance and is an important regulator of memory formation, synaptic plasticity, and structural remodeling (Dana et al., 2020b). Thus, altering autophagy during neurodevelopment and synaptic plasticity can lead to neurodevelopmental disorders by causing abnormal development and synaptic disorder (Lee et al., 2013).

In the literature, several mouse models have been conducted to reveal the link between autophagy and neurodevelopment diseases, including syndromic and VPA models (Lieberman et al., 2020; Sharma et al., 2010; Zhang et al., 2016). *Cc2d1a* knock-out pups die at birth due to respiratory deficits, conditional knock-outs in the cortex and hippocampus leads to cognitive and social deficits, hyperactivity, and anxiety in males (Zamarbide et al., 2019). In *Cc2d1a* animal models, there has been shown to be a lack of neural plasticity, spatial learning, and memory accompanying decreased socialization, hyperactivity, anxiety, and excessive self-care (Oaks et al., 2017). Although sex-specific differences have been reported in this mouse model (Dana et al., 2020b; Zamarbide et al., 2019), more detailed studies are needed to determine the impact of autophagy in neurodevelopment diseases.

Aberration of the autophagy mechanism can lead to abnormal neurological development and dysfunction of synapses in the brain (Deng et al., 2021). In this study, we evidenced altered autophagy in the transgenerational mouse model of *Cc2d1a*. We show sex specific autophagy alteration with aberrant expression of markers (Beclin-1/p62 ratio in the hippocampus) not only in heterozygous *Cc2d1a* mice, but also in (+/+) siblings reminiscent of changes in epigenetic inheritance.

2. Materials and methods

2.1. Study design and animals

We purchased *Cc2d1a* (+/−) mice from the Jackson Laboratory and crossed them with the *Balb-C* background for 10 generations and maintained in our transgenic unit at Erciyes University Genome and Stem Cell Center (GENKOK). *Cc2d1a* (+/−) males were mated with normal (+/+) or heterozygous (+/−) females, successively generating G1 and G2 groups. Further analysis was conducted on groups of two-month-old mice (*n* = 12 for each sex) from all groups, including *Balb-C* controls subjected to behavioral tests. *Cc2d1a* (+/−) crossed with *Balb-C* in group 1 (G1) and *Cc2d1a* (+/−) crossed with *Cc2d1a* (+/−) in group 2 (G2). Controls for all groups are wild type normal Balb/C, which

were never crossed with the mutant mice. The mice were maintained in a facility under controlled conditions (light from 06:00 to 18:00, 22 °C temperature, 55% humidity) in GENKOK. All the animals are followed in the same animal facility and over the same time scale, under well controlled conditions of food, water, temperature, light and care. Always the same persons were allowed to enter the transgenic unit. The animals were cared for and treated according to the Principles of Laboratory Animal Care (European rules). This study was approved by the Erciyes University Animal Ethics Committee of (14.12.2016, 16/151). The experimental design of the study has been summarized in Fig. 1.

2.2. Cc2d1a genotyping

Heterozygotes and wild types were identified by PCR genotyping according to the instructions with the oligonucleotides proposed by Jackson Laboratory according to our previous study (*Ccd1a*-M1: 5′-GTG CGA GGC CAG AGG CCA CTT GTG-3′, *Ccd1a*-M2: 5′-GAC CCT GAG AGA GCT CCT GAG AGC-3′, *Ccd1a*-M3: 5′-TTT CCC ACC TCT TCT GGC CCA GAGG-3′) (Dana et al., 2020b).

2.3. Behavioral tests

In our study, separate groups of mice (G1, G2 and controls, n = 12 mice per group) were used for each test under blind conditions. Each mouse was placed in a separate cage 1 h before the start of the experiments. The experiments were carried out during the light cycle (between 8:00 a.m.-5:00 p.m.). Test arenas were cleaned between trials with 70% ethanol. Animal behavior was videotaped, tracked, and analyzed with EthoVision (Netherlands) video tracking systems. The behavioral tests were performed between 10 a.m. and 4 p.m. in separate rooms. Behavioral tests included as social interaction, novel object recognition, suspension of the mouse by the tail, open field, Y-maze and hole board test.

2.4. Social interaction test

The social interaction test was used to measure sociability and performed as mentioned in our previous study (Ozkul et al., 2020). The test mouse was introduced centrally to initiate habituation for 10 min while blocking access to the side compartments. The first test was conducted by placing an unfamiliar mouse inside an empty wire cage in one of the side chambers to measure the social interaction of the subject mouse without direct social contact. On the other side was an empty wire cage. Each test lasted 10 min and floor surfaces were wiped with 70% ethanol between tests. The accumulated time spent in each compartment and the indices of sociability or social preference were measured to quantify the social behavior of the mice.

2.5. Tail suspension test

The test mouse remained in the room for 15–30 min before starting the experiment. The apparatus used for the tail test consisted of two filter covers each and allowed simultaneous testing of three mice. Each mouse was suspended by the tail from a hook connected to the strain gauge, to which they were attached with 18 cm long tape. The duration of each trial was 6 min. The mouse tail suspension test was recorded using an EthoVision video recorder. After recording, the mice's period of immobility (during which they remained inactive) was calculated. A posture of immobility indicates the abandonment of struggling and depression (Sener et al., 2023; Ozkul et al., 2020). Mice were considered as immobile when they showed dsepair, in which the mice stopped struggling to overcome the abnormal position, and were almost immobile or completely motionless after a period of intense activity. Autistic models have been observed to have less movement and avoidance skills.
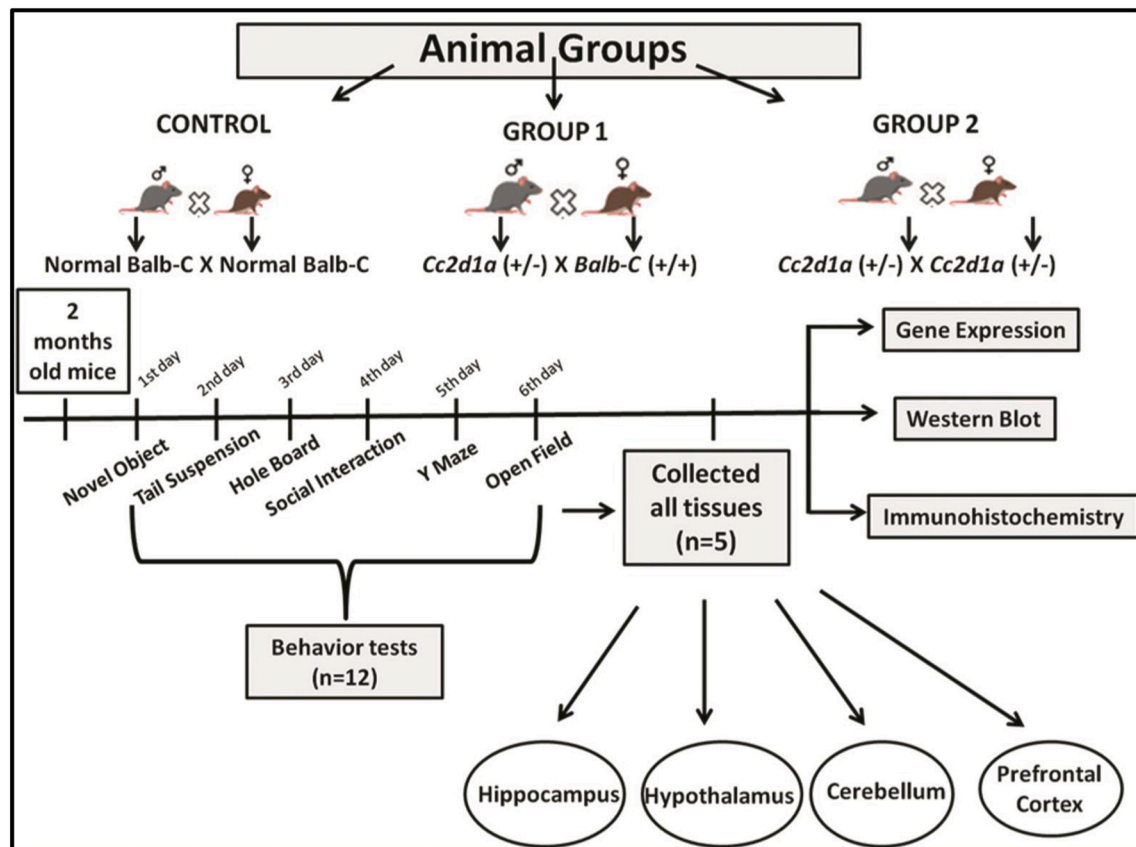
Fig. 1. Schematic illustration of the animal model and timeline for the experiment (detailed description showed in the Materials and Methods).

2.6. Novel object recognition (NOR) test

NOR is a well-established test in a variety of animal models with multiple protocols, indicated differences in interest and object recognition. In general, these are two cognitive assessment tests based on the spontaneous exploratory conduct of a mouse to measure recognition memory. In the first trial, we used (first-day acquisition) animals that were exposed to two similar objects (small orange boxes) in a chamber for 5 min. During the second trial (second-day retention), the mice were again exposed to two different objects for 5 min, including a familiar object from the first trial and a novel object (blue box). Object recognition was measured based on the difference in time spent with the familiar object versus the novel object (Ozkul et al., 2020).

2.7. RNA extraction

Total RNA was prepared from mouse tissues (hippocampus, hypothalamus, cerebellum and prefrontal cortex). Briefly, RNAs were extracted from all tissues via a standard protocol by TRIzol (Roche, Germany) was used according to the manufacturer's instructions. The aqueous phase extracted with TRIzol was precipitated with ethanol, and then washed twice with 70% ethanol. Then the quantity (absorbance at 260 nm) and quality (ratio of absorbance at 260 nm and 280 nm) of the RNA were evaluated with a BioSpec-Nano Spectrophotometer. RNAs were stored at $-80\ ^\circ$C until use.

2.8. Reverse transcription and quantitative real time PCR (QRT-PCR)

Total RNAs were extracted with Trizol reagent (Roche) from dissected brain tissues. RNA concentration was measured with a Nanodrop (Thermo Fisher Scientific). Aliquots of RNA (10 ng) were reverse transcribed into cDNA with the Transcriptor High Fidelity cDNA

Synthesis Kit (Roche). cDNA samples were diluted 1/5 with nuclease free water. qRT-PCR was performed using TaqMan probes (Applied Biosystems) for LC3, Beclin-1, p62; Beta-actin (*Actb*) served as an endogenous reference. Reactions were performed in duplicate in the LightCycler 480 II Real-Time PCR instrument (Roche, Germany). The relative change in mRNA expression was determined by the $2^{-\Delta Ct}$ method.

2.9. Histological analysis

The brain samples collected from the experimental groups were subjected to tissue monitoring steps to be examined by histopathological analysis. Briefly, 5 μm thick sections were taken from tissue samples fixed in 10% formaldehyde solution, embedded in paraffin after passing through increasing series of alcohol (70%, 80%, 96% and 100% ethanol) and stained with Harris Hematoxylin-Eosin (H&E) and light microscopy (Olympus BX53) (Cakir et al., 2019). The presence of degenerated dilated blood vessels and hollow apoptotic cells in the subjects' brain tissues was examined in the cortex, hippocampus and cerebellum.

2.10. Immunohistochemistry analysis

The immunoreactivity of Beclin 1, Lc3A/B, and P62/SQSTM1 proteins in the brain tissues of the experimental groups was determined by the Avidin-Biotin peroxidase method (Cakir et al., 2019). Briefly, after deparaffinization of 5 μm thick sections, they were heated in a 300 W microwave oven in citrate buffer 2 × 4 times (pH: 6.0) to open the epitopes. The preparations were then taken up in a solution of 3% hydrogen peroxide in methanol to inhibit endogenous peroxidase activity. Ultra V block solution was applied to avoid non-specific staining. Sections were then incubated with primary antibodies at 4 °C overnight. Biotinylated streptavidin-HRP and DAB secondary chromogens were

applied, respectively, and sections were counterstained with hematoxylin Gill. It was dehydrated by a series of increasing alcohol and covered with a sealant called entellan. Sections were examined with an Olympus BX53 optical microscope. Evaluation of immunoreactivity levels was performed with the Image J program.

2.11. Western blot

All tissue were homogenized in lysis buffer supplemented with proteinase inhibitors and centrifuged at 12,000 $\times g$ for 10 min at 4 °C to collect cell proteins in the supernatant. Primary neurons were lysed and centrifuged as above, except that the centrifugation took for 5 min. Protein concentrations were measured, and Western blots were performed as described (Hamurcu et al., 2018). Equal amounts of protein aliquots were used to verify target protein expression levels using Lc3 (2775S, Cell Signaling), Beclin-1 (3738S, Cell Signaling), p62 (5114S, Cell Signaling), and beta-actin (4970S, Cell Signaling) by 10% SDS-PAGE gel electrophoresis, and β-actin served as loading control. After incubation with the appropriate HRP-conjugated secondary antibody, proteins were visualized using ECL. Immunoblots density was performed using the hemidoc MP Imaging System (Bio-Rad) and quantified using Quantity One version 4.1.0 (Alpha Innotech, San Leandro, CA). Band densities were normalized to β-actin (as loading control). Band densities were quantified using Image J software. Secondary antibodies used for Western blot included goat anti-rabbit IgG Conjugate (H + L)-HRP (cat. 170–6515, BioRad), Goat Anti-mouse IgG (H + L)-HRP Conjugate (cat. 170–6516, Bio-Rad).

2.12. Statistical analysis

Data are presented as the mean ± standard error of the mean (SEM). The Kolmogorov–Smirnov test was used to analyze the normal distribution of the data. Student's *t*-test (unpaired, two-tailed) was used for two-group comparisons, and two way ANOVA followed by a Tukey's test was used for experiments involving more than two groups. Differences with *p*-values ≤0.05 were considered as significant. The GraphPad Prism program (version 8) was used to evaluate data and graphs.

3. Results

3.1. Offspring of heterozygous Cc2d1a mice show altered phenotype with gender differences

An overview of phenotypic differences according to behavior tests has been summarized in Table 1a. Additionally changes in the expression of autophagy markers were shown in Tables 1b and 1c. Fig. 2F shows the results of the suspension by tail, social interaction and novel object test. Other tests such as Y Maze, Open Field (OF) and Hole Board have been summarized in the Supplemental file (Supplementary Fig. 1A, 1B, 2A, 2B).

Offspring of *Cc2d1a* +/− mice show a significant reduction in movement time in tail suspension assays (Fig. 2A), while their *Cc2d1a* +/+ congeners show higher activity than controls. Male and female control mice in the social interaction tests spent more time at the side of a cage with a live mouse see Fig. 2C and D. In contrast, the three generations established from heterozygous *Cc2d1a* mice behave differently.

Table 1b
Overview of expression changes of autophagy markers in the hippocampus.

| Markers | Male | Female | Male | | Female | |
	Control	Control	*Cc2d1a* +/+	*Cc2d1a* +/−	*Cc2d1a* +/+	*Cc2d1a* +/−
Beclin	++	++	+++	+++	+	++
Lc3	+	+	+	++	++	+
p62	+	++	++	+++	+	++

+ reveals the autophagy marker differences in the groups.

Table 1c
Overview of expression changes of autophagy markers in the prefrontal cortex.

| Markers | Male | Female | Male | | Female | |
	Control	Control	*Cc2d1a* +/+	*Cc2d1a* +/−	*Cc2d1a* +/+	*Cc2d1a* +/−
Beclin	++	++	+++	++	++	+++
Lc3	+	+	++	+	+	+
p62	++	+	+++	++++	++	+

+ reveals the autophagy marker differences in the groups.

Males with *Cc2d1a* heterozygous parents spent more time with the empty cage while their sisters spent more time near the cage containing the live mouse. In the novel object test, the recognition time of the familial and novel object was recorded. All offspring of heterozygous *Cc2d1a* mice spent more time with the novel object than controls (Fig. 2E and F).

3.2. The decrease in the Beclin-1/p62 ratio indicate a dysfunction of autopagy in the hippocampus

The efficiency of autophagy (Agam et al., 2017), is evaluated by the Beclin-1/p62 ratio. A defection in autophagy is observed when a lower value of Beclin-1/p62 is obtained see Table 3a for the hippocampus. Especially in male with heterozygous parents *Cc2d1a* this ratio is much lower than in controls (Fig. 3A). Unlike the hippocampus the Beclin-1/p62 ratios in the prefrontal cortex are unchanged in both sexes (Fig. 3B). Some differences are obtained but which are generally not significant.

3.3. Gene expression analysis

3.3.1. Offspring of Cc2d1a heterozygous mice show altered gene expression of autophagy markers (Lc3, Beclin and p62) in hippocampus and prefrontal cortex

Transcripts

Transcriptional analysis of (*Lc3, Beclin and p62*) is shown in Supplementary Fig. 3A,B,E,F and Table 2a in control females/males and all offspring derived from heterozygous *Cc2d1a* mice. *Lc3* transcripts are detected at higher levels in the hippocampus of female from heterozygous *Cc2d1a* parents. In contrast, *Beclin* transcript levels are significantly decreased compared to the control. Finally, the levels of *p62* transcripts are unchanged compared to the control (Table 2a).

The analysis of the transcripts (*Lc3, Beclin and p62*) at the level of the prefrontal cortex is presented in Supplementary Fig. 4A,B,E,F and Table 2b. Transcriptional alterations are seen in both sexes with a

Table 1a
Overview of phenotypic differences of the groups.

| Phenotype | Male | Female | Male | | Female | |
	Control	Control	*Cc2d1a* +/+	*Cc2d1a* +/−	*Cc2d1a* +/+	*Cc2d1a* +/−
Tail Suspension	+	+	++	++++	+++	+
Social	+	++	+++	++++	++	+++
Novel Object	+	+	++	+++	++	++

+ reveals the behavioral test phenotypes in the groups.
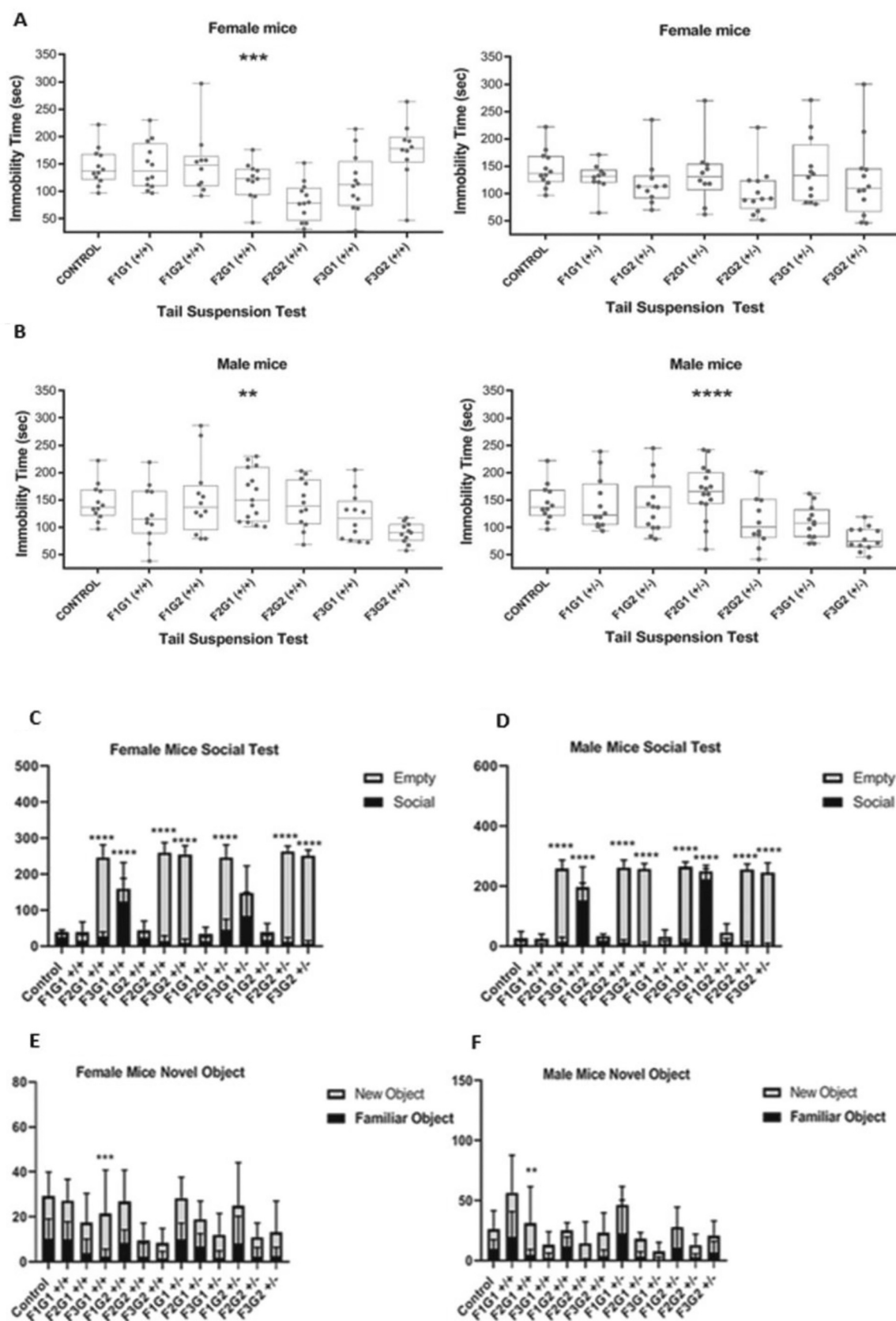
Fig. 2. 2A. Tail Suspension Test for female mice. 2B. Tail Suspension Test for male mice. The immobility time for each group were determined by tail suspension test (TST). Each value represents the mean ± SEM of three independent experiments (control, G1 and G2 n = 12 mice/per group, **** p < 0.0001. 2C. Social test results in female mice. 2D. Social test results in male mice. 2E. Novel object test results in female mice. 2F. Novel object test results in male mice. Each value represents the mean ± SEM of three independent experiments. (control, G1 and G2 *n* = 12 mice/per group), **p < 0.01, ***p < 0.001, **** p < 0.0001.
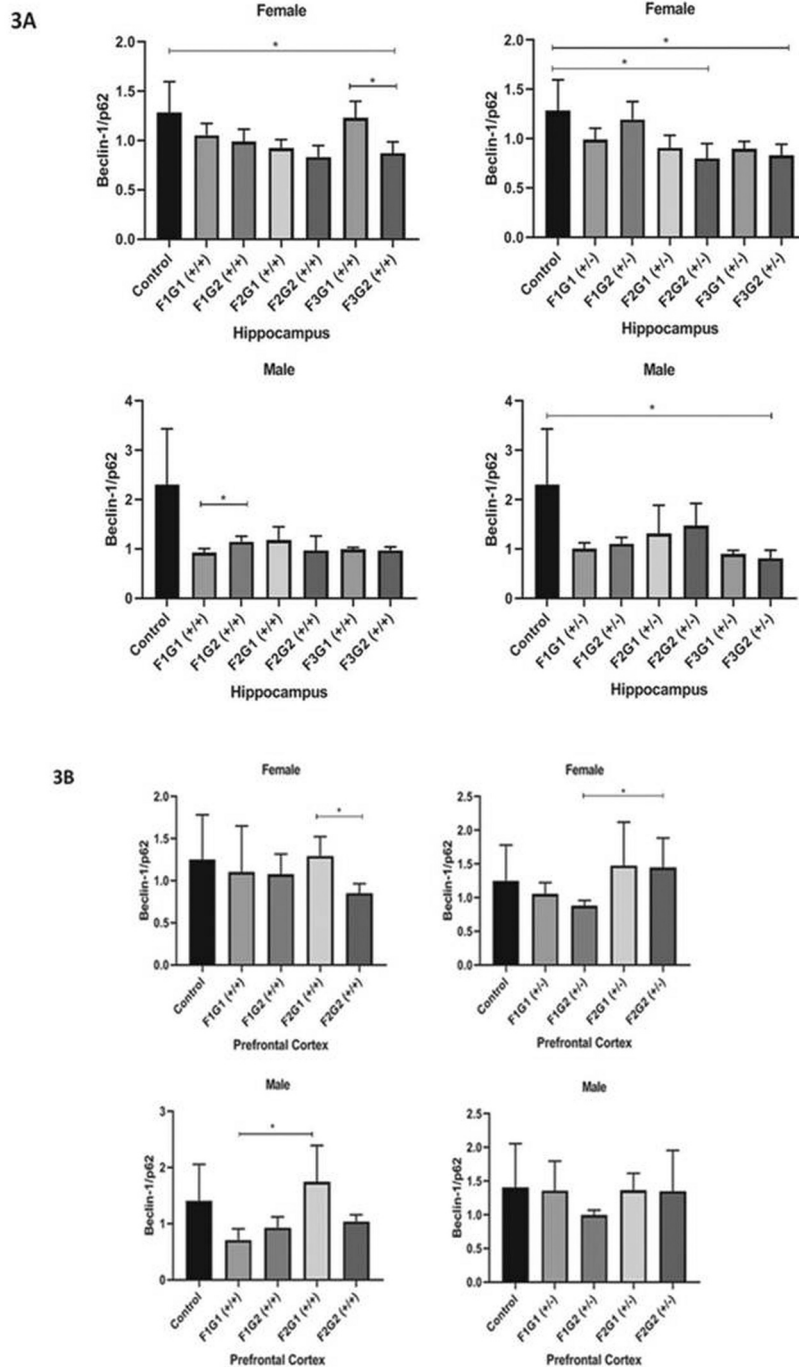
Fig. 3. 3A. Beclin-1/p62 ratio in the hippocampus of each gender. Beclin-1/p62 ratio were established as an indicative measure of autophagy efficiency. When autophagy disrupted the cargo carrier p62 accumulates. Hence Beclin-1/p62 ratio results may be interpreted as deregulated autophagy. Data are presented as means ± SEM. * $p < 0.05$. 3B. Beclin-1/p62 ratio in the prefrontal cortex in each gender. Beclin-1/p62 ratio was established as an indicative measure of autophagy efficiency. When autophagy disrupted the cargo carrier p62 accumulates. Hence Beclin-1/p62 ratio results may be interpreted as deregulated autophagy. Data are presented as means ± SEM. * p < 0.05.

significant decrease in p62, with progeny to progeny variegation in Beclin and some elevation or non change in Lc3 levels.

Transcript analysis from the hypothalamus and cerebellum is summarized in Supplementary table 1 and 2.

Proteins

Proteins analysis (Lc3, Beclin and p62) in the hippocampus is shown in Supplementary Fig. 3C,D,G,H and Table 3a. Significant differences are observed between males and females. While, p62 levels are increased in females, male mice show no significant difference from control. Again, males and females have differences in Beclin expression levels, in fact in females the protein level is increased while in males it is decreased compared to control.

No significant changes were found when comparing Lc3 expression

levels between female groups. (Supplementary Fig. 3D).

Similar to the hippocampus, in the prefrontal cortex Beclin protein expression levels are increased relative to control in both male and female mice of *Cc2d1a* parents (Supplementary Fig. 4C,D,G,H). P62 protein levels are increased in females and unchanged in males. In contrast, Lc3 protein expression levels were lower in females and higher in males compared to controls. Supplementary Fig. 4C,D,G,H and Table 3b show the expression of protein levels in the prefrontal cortex.

Hypothalamus and cerebellum protein analysis summarized in Supplementary table 3 and 4.

Table 2a
Gene expression results of autophagy markers in hippocampus.

Gender/ Genotype	Groups	Gene	Mean	p Value
Female Heterozygote	F2G1 (+/−) vs control	*Lc3*	1.698 ± 0.3629	0.0034 **
Female Heterozygote	F2G2 (+/−) vs control	*Lc3*	0.7650 ± 0.2042	0.0096 **
Female Heterozygote	F2G1 (+/−) vs F2G2 (+/−)	*Lc3*	−0.9325 ± 0.3642	0.0429 *
Female Heterozygote	F1G1 (+/−) vs control	*Beclin*	−0.5775 ± 0.1279	0.0040 **
Female Heterozygote	F1G2 (+/−) vs control	*Beclin*	−0.7925 ± 0.07175	<0.0001 ****
Female Heterozygote	F2G1 (+/−) vs control	*Beclin*	−0.3650 ± 0.1021	0.0117 *
Female Heterozygote	F2G1 (+/−) vs F2G2 (+/−)	*Beclin*	0.3525 ± 0.1087	0.0176 *
Female Heterozygote	F1G1 (+/−) vs control	*P62*	−0.5325 ± 0.1552	0.0186 *
Female Heterozygote	F1G2 (+/−) vs control	*P62*	−0.7850 ± 0.1173	0.0011 **
Female Heterozygote	F2G1 (+/−) vs control	*P62*	−0.5475 ± 0.1194	0.0059 **
Female Heterozygote	F3G2 (+/−) vs control	*P62*	−0.4575 ± 0.1164	0.0111 *
Female Heterozygote	F1G1 (+/−) vs F1G2 (+/−)	*P62*	−0.2525 ± 0.0934	0.0355 *
Female Heterozygote	F2G1 (+/−) vs F2G2 (+/−)	*P62*	0.3425 ± 0.07336	0.0034 **
Female Heterozygote	F3G1 (+/−) vs F3G2 (+/−)	*P62*	−0.3350 ± 0.0748	0.0042 **
Female Normal	F1G2 (+/+) vs control	*Lc3*	1.290 ± 0.4294	0.0239 *
Female Normal	F2G1 (+/+) vs control	*Lc3*	1.730 ± 0.6977	0.0478 *
Female Normal	F2G2 (+/+) vs control	*Lc3*	1.135 ± 0.279	0.0066 **
Female Normal	F1G1 (+/+) vs control	*Beclin*	−0.6975 ± 0.1085	0.0007 ***
Female Normal	F1G1 (+/+) vs F1G2 (+/+)	*Beclin*	0.7275 ± 0.1171	0.0008 ***
Female Normal	F1G1 (+/+) vs F1G2 (+/+)	*P62*	0.6650 ± 0.1631	0.0065 **
Male Heterozygote	F1G1 (+/−) vs control	*Lc3*	0.4200 ± 0.07118	0.0011 **
Male Heterozygote	F1G2 (+/−) vs control	*Lc3*	1.750 ± 0.6356	0.0332 *
Male Heterozygote	F2G1 (+/−) vs control	*Lc3*	0.7975 ± 0.1871	0.0053 **
Male Heterozygote	F3G2 (+/−) vs control	*Lc3*	0.5325 ± 0.1466	0.0109 *
Male Heterozygote	F1G1 (+/−) vs control	*Beclin*	−0.5675 ± 0.08596	0.0006 ***
Male Heterozygote	F2G2 (+/−) vs control	*Beclin*	−0.4975 ± 0.1484	0.0154 *
Male Heterozygote	F3G2 (+/−) vs control	*Beclin*	−0.4225 ± 0.1075	0.0077 **
Male Heterozygote	F3G1 (+/−) vs F3G2 (+/−)	*Beclin*	−0.5825 ± 0.2344	0.0475 *
Male Heterozygote	F1G2 (+/−) vs control	*P62*	−0.4850 ± 0.1260	0.0085 **
Male Heterozygote	F2G2 (+/−) vs control	*P62*	−0.3525 ± 0.1127	0.0204 *
Male Heterozygote	F3G1 (+/−) vs control	*P62*	−0.2325 ± 0.03473	0.0005 ***
Male Heterozygote	F3G2 (+/−) vs control	*P62*	−0.5600 ± 0.02541	<0.0001 ****
Male Heterozygote	F3G1 (+/−) vs F3G2 (+/−)	*P62*	−0.3275 ± 0.04008	0.0002 ***
Male Normal	F1G1 (+/+) vs control	*Lc3*	1.083 ± 0.4359	0.0476 *
Male Normal	F1G2 (+/+) vs control	*Lc3*	0.8800 ± 0.2354	0.0096 **
Male Normal	F1G1 (+/+) vs control	*Beclin*	−0.7425 ± 0.08375	0.0001 ***

Table 2a (*continued*)

Gender/ Genotype	Groups	Gene	Mean	p Value
Male Normal	F2G1 (+/+) vs control	*Beclin*	−0.5775 ± 0.1283	0.0041 **
Male Normal	F3G2 (+/+) vs control	*Beclin*	−0.2325 ± 0.09317	0.0468 *
Male Normal	F1G1 (+/+) vs F1G2 (+/+)	*Beclin*	0.5200 ± 0.1524	0.0143 *
Male Normal	F1G1 (+/+) vs control	*P62*	−0.5875 ± 0.1034	0.0013 **
Male Normal	F2G1 (+/+) vs control	*P62*	−0.4850 ± 0.1493	0.0175 *
Male Normal	F2G2 (+/+) vs control	*P62*	−0.5475 ± 0.1061	0.0021 **
Male Normal	F3G1 (+/+) vs control	*P62*	−0.3425 ± 0.1007	0.0145 *
Male Normal	F1G1 (+/+) vs F1G2 (+/+)	*P62*	0.5525 ± 0.1628	0.0146 *

* p<0.05
** p<0.01
*** p < 0.001.
**** p < 0.0001.

3.4. Immunohistochemistry analysis of expression of autophagy markers (Lc3, Beclin and p62) reveals hippocampus and frontal cortex with sex differences in offspring of Cc2d1a heterozygous parents

Tissues (hippocampus, prefrontal cortex, hypothalamus and cerebellum) are unaffected at histomorphological examination levels in heterozygous *Cc2d1a* offspring compared to controls. Photographs of hematoxylin-eosin staining are shown in Supplementary Fig. 7A,B,C,D.

Immunohistochemical detection of Beclin, Lc3 and P62/SQSTM1 in the hippocampus shows in all groups the difference compared to the control group (Table 4a). Moreover, several differences between females and males are observed in the group with heterozygous *Cc2d1a* parents (Supplementary Fig. 3J and K).

In the prefrontal cortex, the expression of Beclin, Lc3 and P62/SQSTM1 between male and female mice within the groups was similar in the control; whereas there was some sex difference between groups with heterozygous *Cc2d1a* parents (Table 4b, Supplementary Fig. 4J and K). Immunohistochemistry analysis of the cerebellum and hypothalamus summarized in Supplementary table 5 and 6 (Supplementary Fig. 5 K and 5 L, 6A-J).

4. Discussion

Cc2d1a one of several candidate ASD risk genes, is involved in serotonin pathways that converge in the neurobiology of this multifaceted disorder (Pourhamzeh et al., 2021). Mouse models have confirmed the importance of serotonin pathway functions involved in autism. Our results with heterozygous *Cc2d1a* mice define domains of the hippocampus and prefrontal cortex as specifically with impaired autophagy. Increased/decreased autophagy or authophagy imbalance is, among others, one of the factors mediating the etiology of ASD, and previous studies have suggested dysregulation in experimental models of ASD (Lieberman et al., 2020; Yan et al., 2018; Agam et al., 2017; Kim et al., 2017). Our studies examine autophagy parameters in different brain regions of *Cc2d1a*$^{+/−}$ and wild type mice and show the aberrant autophagy mechanism in the hippocampus and altered in the prefrontal cortex of heterozygous offspring. We sought to follow the relationship between the mutation, its transgenerational effects and mutant phenotypes in general and with tissue-specific ways. Notably, we show that in mice carrying the mutation (*Cc2d1a*$^{+/−}$) inherited from different genomic contexts backgrounds, influence phenotypic expressiveness, based on both the autism gene risk and epigenetic inheritance (Ozkul et al., 2020; Dana et al., 2020b). In our previous studies we had observed differences between two lines (C57BL/6 and *Balb/c*) but the *Cc2d1a*

Table 2b
Gene Expression Profiles of autophagy markers in prefrontal cortex.

Gender/Genotype	Groups	Gene	Mean	p Value
Female Heterozygote	F1G2 (+/−) vs control	Lc3	0.9000 ± 0.3061	0.0259 *
Female Heterozygote	F1G1 (+/−) vs control	Beclin	−0.6725 ± 0.1001	0.0005 ***
Female Heterozygote	F1G2 (+/−) vs control	Beclin	−0.3850 ± 0.1388	0.0322 *
Female Heterozygote	F2G1 (+/−) vs control	Beclin	−0.4825 ± 0.1365	0.0123 *
Female Heterozygote	F2G2 (+/−) vs control	Beclin	−0.5150 ± 0.1564	0.0166 *
Female Heterozygote	F3G2 (+/−) vs control	Beclin	−0.4200 ± 0.1171	0.0116 *
Female Heterozygote	F1G1 (+/−) vs control	P62	−0.4625 ± 0.1849	0.0464 *
Female Normal	F1G1 (+/+) vs control	Lc3	1.248 ± 0.3529	0.0123 *
Female Normal	F1G1 (+/+) vs control	Beclin	−0.6350 ± 0.09359	0.0005 ***
Female Normal	F1G2 (+/+) vs control	Beclin	−0.3525 ± 0.1018	0.0134 *
Female Normal	F3G2 (+/+) vs control	Beclin	−0.5800 ± 0.1862	0.0264 *
Female Normal	F1G1 (+/+) vs control	P62	−0.4425 ± 0.1746	0.0444 *
Female Normal	F1G2 (+/+) vs control	P62	−0.4350 ± 0.1614	0.0358 *
Male Heterozygote	F1G2 (+/−) vs control	Lc3	0.7075 ± 0.2480	0.0463 *
Male Heterozygote	F1G1 (+/−) vs control	Beclin	−0.8200 ± 0.1140	0.0004 ***
Male Heterozygote	F2G1 (+/−) vs control	Beclin	−0.4375 ± 0.1418	0.0215 *
Male Heterozygote	F2G2 (+/−) vs control	Beclin	−0.5433 ± 0.1597	0.0192 *
Male Heterozygote	F1G1 (+/−) vs control	P62	−0.7750 ± 0.1218	0.0007 ***
Male Heterozygote	F1G2 (+/−) vs control	P62	−0.7325 ± 0.1199	0.0009 ***
Male Heterozygote	F2G1 (+/−) vs control	P62	−0.5750 ± 0.1297	0.0044 **
Male Heterozygote	F3G1 (+/−) vs control	P62	−0.4050 ± 0.09962	0.0066 **
Male Heterozygote	F3G2 (+/−) vs control	P62	−0.5425 ± 0.08707	0.0008 ***
Male Heterozygote	F3G1 (+/−) vs F3G2 (+/−)	P62	−0.1375 ± 0.05186	0.0380 *
Male Normal	F1G2 (+/+) vs control	Lc3	1.005 ± 0.3130	0.0183 *
Male Normal	F2G1 (+/+) vs control	Lc3	1.198 ± 0.2953	0.0067 **
Male Normal	F2G1 (+/+) vs F2G2 (+/+)	Lc3	−1.240 ± 0.2872	0.0050 **
Male Normal	F1G1 (+/+) vs control	Beclin	−0.8300 ± 0.1075	0.0002 ***
Male Normal	F1G2 (+/+) vs control	Beclin	−0.2750 ± 0.09412	0.0266 *
Male Normal	F2G1 (+/+) vs control	Beclin	−0.4300 ± 0.1319	0.0173 *
Male Normal	F2G2 (+/+) vs control	Beclin	−0.3475 ± 0.1090	0.0189 *
Male Normal	F1G1 (+/+) vs F1G2 (+/+)	Beclin	0.5550 ± 0.08391	0.0006 ***
Male Normal	F1G1 (+/+) vs control	P62	−0.8200 ± 0.09857	0.0002 ***
Male Normal	F1G2 (+/+) vs control	P62	−0.4000 ± 0.08803	0.0039 **
Male Normal	F2G1 (+/+) vs control	P62	−0.7000 ± 0.1012	0.0005 ***
Male Normal	F3G1 (+/+) vs control	P62	−0.3750 ± 0.09287	0.0068 **
Male Normal	F3G2 (+/+) vs Control	P62	−0.4375 ± 0.1064	0.0063 **
Male Normal	F1G1 (+/+) vs F1G2 (+/+)	P62	0.4200 ± 0.05148	0.0002 ***
Male Normal	F2G1 (+/+) vs F2G2 (+/+)	P62	0.6625 ± 0.1139	0.0011 **

* p < 0.05.
** p < 0.01.
*** p < 0.001.

mutation or the VPA treatment induced autism-like changes in the two lines of mice. In current studies and previous reports (Sener et al., 2023; Ozkul et al., 2020; Dana et al., 2020a, 2020b), we used the *Balb/c* lineage and here we only consider the differences induced by the *Cc2d1a* mutation compared to wild type. Our results shows that different cross-types background with a single autism gene risk, in heterozygous parents with a consistent genetic background converge to a variable autism-like phenotype, even in offspring with a wild-type genotype but altered autophagy phenotype. This suggests that a common clinical pathology may derive during differentiation of biological process due to altered genes in progenitors. These findings direct future research plan toward therapeutic approaches with variable alteration in autophagy activities in addition to shared molecular pathways. This is important information, as many patients with behavior disorders have varying clinical manifestations.

CC2D1A is a ubiquitously expressed multifunctional protein with repressor activities at the serotonin-1A receptor (HTR1A) that regulates several intracellular pathways critical for neuronal function. Postnatal forebrain elimination of *Cc2d1a* in mice (conditional knock-out) is observed by behavioral changes in the male recapitulating several features of ASD and ID including hyperactivity, social and cognitive deficits, increased anxiety-like behaviors and obsessive grooming (Yang et al., 2019; Oaks et al., 2017). However, female mice are less severely affected, showing only obsessive grooming and object recognition deficit, but show normal spatial memory in the Morris Water Maze, normal social function, and activity levels (Mossa and Manzini, 2019). Many behavioral tests are proposed, here the descendants of $Cc2d1a^{+/−}$ show notable differences with the control with recognition of novel objects, social area and suspended by the tail. We showed that sex differences were particularly reflected in suspension by tail and novel object tests with more significant differences in male mice. Behavioral screening is important because of the genetic and phenotypic variability of behavior disorders. It is already known that the identified behavioral deficits are predominantly specific to men, but there are also modifications specific to women depending on age, genetic, and behavioral test (Mossa and Manzini, 2019). For example, female patients show frequently low intellectual level and greater internalizing symptoms compared to male patients with greater social and externalizing behavioral problems, such as aggressive behaviors and increased repetitive stereotyped behaviors (Baio et al., 2018; Iossifov et al., 2014; Werling, 2016).

Although, it is still very mysterious, analysis of neuroimage acquisition seem to indicate sex specifc differences, in the motor system and in areas of the "social brain" (Lombardo et al., 2020). More importantly, the fetal testosterone level is correlated with the gender difference in ASD (Auyeung et al., 2009). For example, FOXP1, a male-specific gene, is influenced by estrogen dihydrotestosterone alteration that acts via androgen receptor to influence gene expression in human neural stem cells (Lombardo et al., 2020). TCF4, a female specific gene, play an important role in nervous system development (Forrest et al., 2018) and participate in the androgen receptor activity (Heemers and Tindall, 2007).

Finally, analysis of gene expression linked to autism by sex difference highlights the greater amount of co-expressed genes in women than men which supports "a female protective effect" (Mossa and Manzini, 2019).

Autophagy is a highly dynamic process that occurs in multiple steps, increased amounts of LC3-II may reflect autophagosome accumulation resulting from reduced autophagosome turnover as well as in the case of inefficient fusion with endosomes and/or lysosomes. When fusion occurs, it causes inefficient degradation of the cargo. Beclin-1 is part of the PI3KC3 (phosphatidylinositol 3-kinase catalytic subunit type 3)

Table 3a
Western results of autophagy markers in hippocampus.

Gender/ Genotype	Groups	Gene	Mean	p Value
Female Heterozygote	F1G1 (+/−) vs control	Lc3	−0.7878 ± 0.2733	0.0280 *
Female Heterozygote	F3G2 (+/−) vs control	Lc3	−0.6603 ± 0.2569	0.0423 *
Female Heterozygote	F1G1 (+/−) vs F1G2 (+/−)	Lc3	0.3939 ± 0.1293	0.0226 *
Female Heterozygote	F3G1 (+/−) vs F3G2 (+/−)	Lc3	−2.386 ± 0.8655	0.0330 *
Female Heterozygote	F1G1 (+/−) vs F1G2 (+/−)	Beclin	0.3337 ± 0.1151	0.0274 *
Female Heterozygote	F2G2 (+/−) vs control	P62	0.3844 ± 0.1498	0.0426 *
Female Heterozygote	F2G1 (+/−) vs F2G2 (+/−)	P62	0.2925 ± 0.1131	0.0414 *
Female Heterozygote	F2G2 (+/−) vs control	Beclin / P62	−0.4873 ± 0.1730	0.0426 *
Female Heterozygote	F3G2 (+/−) vs control	Beclin / P62	−0.4576 ± 0.1659	0.0414 *
Female Normal	F2G1 (+/+) vs F2G2 (+/+)	Beclin	0.3949 ± 0.1431	0.0329 *
Female Normal	F2G2 (+/−) vs control	Beclin / P62	−0.4546 ± 0.1662	0.0339 *
Female Normal	F3G2 (+/−) vs control	Beclin / P62	−0.4163 ± 0.1660	0.0461 *
Female Normal	F3G1 (+/−) vs F3G2 (+/−)	Beclin / P62	−0.3592 ± 0.1029	0.0130 *
Male Heterozygote	F1G1 (+/−) vs control	Beclin	−2.042 ± 0.6270	0.0173 *
Male Heterozygote	F1G2 (+/−) vs control	Beclin	−1.959 ± 0.6225	0.0199 *
Male Heterozygote	F2G1 (+/−) vs control	Beclin	−2.169 ± 0.6325	0.0140 *
Male Heterozygote	F3G1 (+/−) vs control	Beclin	−1.848 ± 0.6430	0.0283 *
Male Heterozygote	F3G2 (+/−) vs control	Beclin	−2.035 ± 0.6260	0.0175 *
Male Heterozygote	F2G1 (+/−) vs F2G2 (+/−)	Beclin	0.9245 ± 0.3674	0.0455 *
Male Heterozygote	F2G1 (+/−) vs F2G2 (+/−)	P62	0.4823 ± 0.1874	0.0421 *
Male Heterozygote	F3G2 (+/−) vs control	Beclin / P62	−1.492 ± 0.5544	0.0432 *
Male Normal	F1G1 (+/+) vs control	Lc3	1.083 ± 0.4359	0.0476 *
Male Normal	F1G2 (+/+) vs control	Lc3	0.8800 ± 0.2354	0.0096 **
Male Normal	F2G1 (+/+) vs control	Lc3	−0.2400 ± 0.07012	0.0141 *
Male Normal	F1G1 (+/+) vs control	Beclin	−0.7425 ± 0.08375	0.0001 ***
Male Normal	F2G1 (+/+) vs control	Beclin	−0.5775 ± 0.1283	0.0041 **
Male Normal	F3G2 (+/+) vs control	Beclin	−0.2325 ± 0.09317	0.0468 *
Male Normal	F1G1 (+/+) vs F1G2 (+/+)	Beclin	0.5200 ± 0.1524	0.0143 *
Male Normal	F1G1 (+/+) vs control	P62	−0.5875 ± 0.1034	0,0013 **
Male Normal	F2G1 (+/+) vs control	P62	−0.4850 ± 0.1493	0,0175 *
Male Normal	F2G2 (+/+) vs control	P62	−0.5475 ± 0.1061	0,0021 **
Male Normal	F3G1 (+/+) vs control	P62	−0.3425 ± 0.1007	0,0145 *
Male Normal	F3G2 (+/+) vs control	P62	0.3600 ± 0.1332	0,0354 *
Male Normal	F1G1 (+/+) vs F1G2 (+/+)	P62	0.5525 ± 0.1628	0,0146 *

* * p < 0.05.
** ** p < 0.01.
*** *** p < 0.001.

Table 3b
Western results of autophagy markers in prefrontal cortex.

Gender/ Genotype	Groups	Gene	Mean	p Value
Female Heterozygote	F1G2 (+/−) vs control	Lc3	0.5112 ± 0.1434	0.0119 *
Female Heterozygote	F2G1 (+/−) vs control	Lc3	0.9284 ± 0.2340	0.0074 **
Female Heterozygote	F2G2 (+/−) vs control	Lc3	0.5986 ± 0.1713	0.0129 *
Female Heterozygote	F2G1 (+/−) vs F2G2 (+/−)	Beclin	0.2713 ± 0.09014	0.0237 *
Female Normal	F1G2 (+/+) vs control	Lc3	0.3395 ± 0.1322	0.0425 *
Female Normal	F2G1 (+/+) vs control	Lc3	0.8727 ± 0.2162	0.0068 **
Female Normal	F2G1 (+/−) vs F2G2 (+/−)	Beclin / P62	−0.4429 ± 0.1284	0.0136 *
Male Normal	F2G2 (+/+) vs control	Lc3	0.9427 ± 0.3346	0.0305 *
Male Normal	F2G1 (+/+) vs control	Beclin	0.5371 ± 0.1923	0.0314 *

* p < 0.05.
** p < 0.01.

autophagy initiator complex that regulates autophagosome synthesis downstream of the mTOR independent pathway. Beclin-1 (encoded by BECN1) is therefore elevated when autophagy develops. p62 (also known as SQSTM1, a ubiquitin-binding scaffold protein) is degraded during the process of autophagy and therefore its levels decrease when autophagy is induced (Agam et al., 2017; Sade et al., 2016).

Cc2d1a is also a regulator of Akt signaling (Nakamura et al., 2008) and therefore it is plausible that *Cc2d1a* deficiency may modulate the PI3K/Akt/mTor pathway leading to similar physiological and behavioral outcomes (Oaks et al., 2017). mTOR is a central regulator of diverse cellular processes including autophagy and is negatively regulated by tuberous sclerosis complex 1/2 (TSC1/2) (Deng et al., 2021; Kim et al., 2011). A previous study reported that TSC2 +/− mice exhibit constitutive hyperactivity, autophagy blockade, and resultant spinal pruning defects (Tang et al., 2014). In addition to TSC1/2 models of ASD, recent studies have reported altered expression of the autophagy related protein Beclin-1 in animal models of ASD including *Cc2d1a* (intracellular signaling) and *ADNP* (chromatin remodeling) deficient mice (Dana et al., 2020b; Amram et al., 2016). In hippocampal samples from *Cc2d1a* [+/−] mice Beclin-1 and Lc3 expressions were generally increased for females and decreased for males compared to their controls (Dana et al., 2020b). These studies indicate that dysregulation of autophagy may contribute to neuronal pathology and aberrant social behaviors. Another study showed that biochemical markers of autophagy such as LC3-II, the active form of p-ULK1 and p-Beclin-1, and the resulting autophagy flux are significantly reduced, while p62 accumulates in the hippocampal neurons of *Fmr1*-KO mice as a result of aberrant mTOR signaling (Yan et al., 2018). These results indicate that mTOR-dependent autophagy is impaired in FXS and that activation of autophagy by mTOR inhibition prevents neuronal deficits in FXS.

When autophagy is suppressed or interrupted, the cargo carrier p62 accumulates. The Beclin-1/p62 ratio is currently used as a coalesced marker of autophagy efficiency (Agam et al., 2017). Therefore, the increase in the Beclin-1/p62 ratio suggests an increase in autophagy. The combined levels of Beclin-1 and p62 levels and the Beclin-1/p62 ratio results can be interpreted as reduced autophagy in *Cc2d1a*^{+/−} mice. In our previous report on *Cc2d1a*^{+/−} mice, Beclin-1 expression levels in the hippocampus were significantly decreased. Here, a marked decrease in the Beclin-1/p62 ratio was observed in the hippocampus, while a more fluctuating state was observed in the prefrontal cortex, and a more evident decrease was observed in male mice. Together, the Beclin-1/p62 ratio and expression levels indicate reduced autophagy in the hippocampus and prefrontal cortex of these mice.

Table 4a

Immunohistochemistry results of autophagy markers in hippocampus.

Gender/Genotype	Groups	Gene	Mean	p Value
Female Heterozygote	F1G1 (+/−) vs F1G2 (+/−)	*Lc3*	5.102 ± 0.2177	0.0018 **
Female Heterozygote	F2G1 (+/−) vs F2G2 (+/−)	*Lc3*	−3.913 ± 0.1180	0.0009 ***
Female Heterozygote	F3G1 (+/−) vs F3G2 (+/−)	*Lc3*	4.204 ± 0.3162	0.0056 **
Female Heterozygote	F1G2 (+/−) vs control	*Beclin*	−7.116 ± 0.5839	0.0067 **
Female Heterozygote	F2G2 (+/−) vs control	*Beclin*	−7.588 ± 0.5092	0.0045 **
Female Heterozygote	F2G1 (+/−) vs F2G2 (+/−)	*Beclin*	7.793 ± 0.1870	0.0006 ***
Female Heterozygote	F2G2 (+/−) vs control	*P62*	8.655 ± 0.4134	0.0023 **
Female Heterozygote	F3G1 (+/−) vs control	*P62*	−7.346 ± 0.4956	0.0045 **
Female Heterozygote	F3G2 (+/−) vs control	*P62*	11.83 ± 0.1809	0.0002 ***
Female Heterozygote	F1G1 (+/−) vs F1G2 (+/−)	*P62*	7.876 ± 0.5484	0.0048 **
Female Heterozygote	F3G1 (+/−) vs F3G2 (+/−)	*P62*	−19.17 ± 0.4908	0.0007 ***
Female Normal	F2G2 (+/+) vs control	*Lc3*	6.161 ± 0.5313	0.0074 **
Female Normal	F3G2 (+/+) vs control	*Lc3*	−6.888 ± 0.5407	0.0061 **
Female Normal	F1G1 (+/+) vs F1G2 (+/+)	*Lc3*	2.815 ± 0.1400	0.0025 **
Female Normal	F2G1(+/+) vs F2G2 (+/+)	*Lc3*	−9.153 ± 0.5260	0.0033 **
Female Normal	F3G1 (+/+) vs F3G2 (+/+)	*Lc3*	6.223 ± 0.3239	0.0027 **
Female Normal	F1G1 (+/+) vs control	*P62*	8.860 ± 0.1679	0.0004 ***
Female Normal	F2G1 (+/+) vs control	*P62*	8.083 ± 0.1466	0.0003 ***
Female Normal	F2G2 (+/+) vs control	*P62*	10.97 ± 0.2175	0.0004 ***
Female Normal	F3G2 (+/+) vs control	*P62*	15.77 ± 0.3836	0.0006 ***
Female Normal	F2G1 (+/+) vs F2G2 (+/+)	*P62*	−2.883 ± 0.1772	0.0038 **
Male Heterozygote	F1G2 (+/−) vs control	*Beclin*	−3.492 ± 0.1754	0.0025 **
Male Heterozygote	F2G1 (+/−) vs control	*Beclin*	2.706 ± 0.09823	0.0013 **
Male Heterozygote	F2G2 (+/−) vs control	*Beclin*	−8.379 ± 0.1303	0.0002 ***
Male Heterozygote	F3G1 (+/−) vs control	*Beclin*	2.463 ± 0.2108	0.0072 **
Male Heterozygote	F3G2 (+/−) vs control	*Beclin*	6.413 ± 0.3615	0.0032 **
Male Heterozygote	F2G1 (+/−) vs F2G2 (+/−)	*Beclin*	11.08 ± 0.1603	0.0002 ***
Male Heterozygote	F1G1 (+/−) vs control	*P62*	4.254 ± 0.4064	0.0090 **
Male Heterozygote	F2G1 (+/−) vs control	*P62*	14.11 ± 0.4757	0.0011 **
Male Heterozygote	F3G2 (+/−) vs control	*P62*	8.353 ± 0.4021	0.0023 **
Male Heterozygote	F2G1 (+/−) vs F2G2 (+/−)	*P62*	13,21 ± 0.4425	0.0011 **
Male Heterozygote	F3G1 (+/−) vs F3G2 (+/−)	*P62*	−5.206 ± 0.4376	0.0070 **
Male Normal	F1G1 (+/+) vs control	*Lc3*	−3.906 ± 0.3175	0.0072 **
Male Normal	F3G1 (+/+) vs control	*Lc3*	4.089 ± 0.3594	0.0076 **
Male Normal	F1G1 (+/+) vs F1G2 (+/+)	*Lc3*	−4.982 ± 0.2583	0.0027 **
Male Normal	F2G1(+/+) vs F2G2 (+/+)	*Lc3*	4.891 ± 0.5988	0.0147 **

Table 4a (*continued*)

Gender/Genotype	Groups	Gene	Mean	p Value
Male Normal	F2G2 (+/+) vs control	*Beclin*	−11.22 ± 0.02532	<0.0001 ****
Male Normal	F3G1 (+/+) vs control	*Beclin*	7.772 ± 0.05405	<0.0001 ****
Male Normal	F3G2 (+/+) vs control	*Beclin*	7.728 ± 0.06626	<0.0001 ****
Male Normal	F2G1(+/+) vs F2G2 (+/+)	*Beclin*	13.48 ± 0.3558	0.0007 ***
Male Normal	F1G1 (+/+) vs control	*P62*	4.252 ± 0.4133	0.0093 **
Male Normal	F1G2 (+/+) vs control	*P62*	6.096 ± 0.5660	0.0085 **
Male Normal	F2G1 (+/+) vs control	*P62*	9.472 ± 0.3598	0.0014 **
Male Normal	F3G1(+/+) vs control	*P62*	5.515 ± 0.3543	0.0041 **
Male Normal	F2G1 (+/+) vs F2G2 (+/+)	*P62*	11.98 ± 0.1056	<0.0001 ****
Male Normal	F3G1 (+/+) vs F3G2 (+/+)	*P62*	5.007 ± 0.05064	0.0001 ***

** p < 0.01.
*** p < 0.001.
**** p < 0.0001.

With transgenerational studies, we assess the severity of autistic phenotypes by creating two different groups and offspring (+/− or +/+) over three generations. All progeny groups were found to be aggressive and hyperactive compared to controls. Expression levels of *Lc3* and *Beclin* transcripts and protein in hippocampal tissues of male and female mice in both groups were altered compared to controls. Overall decreases were observed in autophagy levels. With this study we show a transgenerational variation of autophagy with different genotypes.

Single gene alteration studies of behavioral diseases can be appropriately modeled in mice and have in fact generated important mechanistic information for a better understanding of pathogenesis (Hui et al., 2020). Additionally, since many neuropsychiatric disorders are circuitry disorders, "mouse models" are useful in linking genes to behaviors (Golden et al., 2018; Del Pino et al., 2018). Based on our data, we can suggest that autophagy is differentially regulated in *Cc2d1a* +/− mice, taking into account genotypic siblings and gender differences. Considering the efficiency of autophagy (Agam et al., 2017) the lower value of the Beclin-1/p62 ratio in the hippocampus of male compared to females (Table 3a), we suggest that the mechanism of autophagy is more disrupted and differentiated especially in the male mice.

Moreover, a previous report (Zamarbide et al., 2019) already indicates a specific spatial memory deficit in *Cc2d1a*-deficient male mice. *Cc2d1a* regulates intracellular cAMP signaling in a male-specific manner in the hippocampus and establishes a sex bias in neurodevelopmental disorders. Additionally, in human patients, haploinsufficiency in genes involved in mechanisms such as intracellular signaling (CC2D1A and ERK1) leads to more severe behavioral outcomes in men (Zhang et al., 2020). Thus, the absence of behavioral deficits in females is would be due to compensation mechanisms and cellular functions in both sexes. Here, we reveal higher autophagy dysregulation in male mice that may be part of autism-related cellular dysfunction.

This study proves the heritability of *Cc2d1a* $^{+/-}$ autistic traits with and without DNA mutation inheritance an important knowledge that is not always accessible with human studies.

Funding

Table 4b

Immunohistochemistry results of autophagy markers in prefrontal cortex.

Gender/Genotype	Groups	Gene	Mean	p Value
Female Heterozygote	F1G1 (+/−) vs control	*Lc3*	2.056 ± 0,3404	0.0263 *
Female Heterozygote	F2G2 (+/−) vs control	*Lc3*	5.167 ± 0,3310	0.0041 **
Female Heterozygote	F3G2 (+/−) vs control	*Lc3*	6.553 ± 0,3721	0.0032 **
Female Heterozygote	F3G1 (+/−) vs F3G2 (+/−)	*Lc3*	−9.495 ± 0,2849	0.0009 ***
Female Heterozygote	F1G1 (+/−) vs control	*Beclin*	−2.617 ± 0.4855	0.0327 *
Female Heterozygote	F2G2 (+/−) vs control	*Beclin*	8.592 ± 0.3711	0.0019 **
Female Heterozygote	F2G2 (+/−) vs control	*P62*	5.622 ± 0.3774	0.0045 **
Female Heterozygote	F3G1 (+/−) vs control	*P62*	−2.111 ± 0.1441	0.0046 **
Female Heterozygote	F3G2 (+/−) vs control	*P62*	5.642 ± 0.2536	0.0020 **
Female Heterozygote	F2G1 (+/−) vs F2G2 (+/−)	*P62*	−5.911 ± 0.4501	0.0057 **
Female Heterozygote	F3G1 (+/−) vs F3G2 (+/−)	*P62*	−7.753 ± 0.2506	0.0010 **
Female Normal	F1G2 (+/+) vs control	*Lc3*	9.021 ± 0.4079	0.0020 **
Female Normal	F2G1 (+/+) vs control	*Lc3*	7.200 ± 0.6694	0.0085 **
Female Normal	F3G2 (+/+) vs control	*Lc3*	7.076 ± 0.3145	0.0020 **
Female Normal	F1G1 (+/+) vs F1G2 (+/+)	*Lc3*	−9.151 ± 0.4413	0.0023 **
Female Normal	F3G1 (+/+) vs F3G2 (+/+)	*Lc3*	−5.488 ± 0.2890	0.0028 **
Female Normal	F2G1 (+/+) vs control	*Beclin*	8.542 ± 0.3531	0.0017 **
Female Normal	F2G2 (+/+) vs control	*Beclin*	5.457 ± 0.5176	0.0089 **
Female Normal	F3G1 (+/+) vs control	*Beclin*	5.409 ± 0.4695	0.0075 **
Female Normal	F1G2 (+/+) vs control	*P62*	3.895 ± 0.1558	0.0016 **
Female Normal	F2G1 (+/+) vs control	*P62*	2.060 ± 0.1148	0.0031 **
Female Normal	F2G2 (+/+) vs control	*P62*	4.709 ± 0.2953	0.0039 **
Female Normal	F3G2 (+/+) vs control	*P62*	6.547 ± 0.4491	0.0047 **
Female Normal	F3G1 (+/−) vs F3G2 (+/−)	*P62*	−7.954 ± 0.5183	0.0042 **
Male Heterozygote	F2G1 (+/−) vs control	*Lc3*	−4.096 ± 0.6390	0.0235 *
Male Heterozygote	F3G1 (+/−) vs control	*Lc3*	−6.935 ± 0.4171	0.0036 **
Male Heterozygote	F3G2 (+/−) vs control	*Lc3*	3.297 ± 0.4243	0.0162 *
Male Heterozygote	F1G1 (+/−) vs F1G2 (+/−)	*Lc3*	1.953 ± 0.2536	0.0164 *
Male Heterozygote	F2G1 (+/−) vs F2G2 (+/−)	*Lc3*	−3.263 ± 0.5472	0.0270 *
Male Heterozygote	F3G1 (+/−) vs F3G2 (+/−)	*Lc3*	−10.23 ± 0.3572	0.0012 **
Male Heterozygote	F1G2 (+/+) vs control	*Beclin*	8.039 ± 0.4866	0.0036 **
Male Heterozygote	F2G1 (+/+) vs control	*Beclin*	3.330 ± 0.6823	0.0395 *
Male Heterozygote	F2G2 (+/+) vs control	*Beclin*	8.518 ± 0.3856	0.0020 **
Male Heterozygote	F3G1 (+/+) vs control	*Beclin*	−4.015 ± 0.6183	0.0229 *
Male Heterozygote	F3G2 (+/+) vs control	*Beclin*	6.210 ± 0.8915	0.0200 *
Male Heterozygote	F1G1 (+/+) vs F1G2 (+/+)	*Beclin*	−10.35 ± 0.5713	0.0030 **
Male Heterozygote	F2G1 (+/−) vs F2G2 (+/−)	*Beclin*	−5.188 ± 0.6187	0.0139 *

Table 4b (*continued*)

Gender/Genotype	Groups	Gene	Mean	p Value
Male Heterozygote	F3G1 (+/−) vs F3G2 (+/−)	*Beclin*	−10.22 ± 0.9724	0.0089 **
Male Heterozygote	F1G1 (+/−) vs control	*P62*	−1.793 ± 0.3578	0.0376 *
Male Heterozygote	F2G1 (+/−) vs control	*P62*	−8.759 ± 0.4479	0.0026 **
Male Heterozygote	F3G1 (+/−) vs control	*P62*	−5.169 ± 0.3000	0.0034 **
Male Heterozygote	F3G2 (+/−) vs control	*P62*	3.352 ± 0.2285	0.0046 **
Male Heterozygote	F2G1 (+/−) vs F2G2 (+/−)	*P62*	−5.996 ± 1.014	0.0274 *
Male Heterozygote	F3G1 (+/−) vs F3G2 (+/−)	*P62*	−8.520 ± 0.3019	0.0013 **
Male Normal	F1G2 (+/+) vs control	*Beclin*	8.949 ± 0.5549	0.0038 **
Male Normal	F2G1 (+/+) vs control	*Beclin*	3.369 ± 0.4164	0.0149 *
Male Normal	F2G2 (+/+) vs control	*Beclin*	−4.352 ± 0.8165	0.0334 *
Male Normal	F3G1 (+/+) vs control	*Beclin*	7.991 ± 0.3815	0.0023 **
Male Normal	F3G2 (+/+) vs control	*Beclin*	5.459 ± 0.4359	0.0063 **
Male Normal	F1G1 (+/+) vs F1G2 (+/+)	*Beclin*	−10.58 ± 0.7010	0.0044 **
Male Normal	F2G1 (+/−) vs F2G2 (+/−)	*Beclin*	7.682 ± 0.9491	0.0149 *
Male Normal	F3G1 (+/−) vs F3G2 (+/−)	*Beclin*	2.532 ± 0.3228	0.0159 *
Male Normal	F1G1 (+/+) vs control	*P62*	−3.294 ± 0.2370	0.0051 **
Male Normal	F3G1 (+/+) vs control	*P62*	−7.108 ± 0.4404	0.0038 **
Male Normal	F1G1 (+/+) vs F1G2 (+/+)	*P62*	−3.896 ± 0.4082	0.0108 *
Male Normal	F3G1 (+/+) vs F3G2 (+/+)	*P62*	−7.150 ± 0.4838	0.0045 **

* $p < 0.05$.
** $p < 0.01$.

Authors' contribution

EFS, ZH and ST conceptualized the project; EFS, HD, RT, ND, ZY, EM, ET, ZD, AO, FD performed experiments; EFS, HD, ST, ZH, ZD, YO and MR analyzed data; EFS, HD and ZH wrote the manuscript, MR Writing–Review&Editing.

Ethical statements

All authors analyzed the results and approved the final version of the manuscript.

Declaration of Competing Interest

The authors have no conflicts of interest or other disclosures to report.

Data availability

Data will be made available on request.

Appendix A. Supplementary data

Supplementary data to this article can be found online at https://doi.org/10.1016/j.pnpbp.2023.110764.

References

Agam, G., Taylor, Z., Vainer, E., Golan, H.M., 2017. The influence of choline treatment on behavioral and neurochemical autistic-like phenotype in Mthfr-deficient mice. Transl. Psychiatry 10 (1), 316.

Amram, N., Hacohen-Kleiman, G., Sragovich, S., Malishkevich, A., Katz, J., Touloumi, O., et al., 2016. Sexual divergence in microtubule function: the novel intranasal microtubule targeting SKIP normalizes axonal transport and enhances memory. Mol. Psychiatry 21, 1467–1476.

Auyeung, B., Baron-Cohen, S., Ashwin, E., Knickmeyer, R., Taylor, K., Hackett, G., Hines, M., 2009. Fetal testosterone predicts sexually differentiated childhood behavior in girls and in boys. Psychol. Sci. 20 (2), 144–148.

Baio, J., Wiggins, L., Christensen, D.L., Maenner, M.J., Daniels, J., Warren, Z., Kurzius-Spencer, M., Zahorodny, W., et al., 2018. Prevalence of autism Spectrum disorder among children aged 8 years - autism and developmental disabilities monitoring network, 11 sites, United States. MMWR Surveill Summ. 67 (6), 1–23.

Baribeau, D., Anagnostou, E., 2022. Novel treatments for autism spectrum disorder based on genomics and systems biology. Pharmacol. Ther. 230, 107939.

Basel-Vanagaite, L., Attia, R., Yahav, M., Ferland, R.J., Anteki, L., Walsh, C.A., et al., 2006. The CC2D1A, a member of a new gene family with C2 domains, is involved in autosomal recessive non-syndromic mental retardation. J. Med. Genet. 43, 203–210.

Cakir, M., Tekin, S., Doğanyiğit, Z., Erden, Y., Soytürk, M., Çiğremiş, Y., Sandal, S., 2019. Cannabinoid type 2 receptor agonist JWH-133, attenuates Okadaic acid induced spatial memory impairment and neurodegeneration in rats. Life Sci. 217, 25–33.

Calderoni, S., 2022. Sex/gender differences in children with autism spectrum disorder: a brief overview on epidemiology, symptom profile, and neuroanatomy. J. Neurosci. Res. https://doi.org/10.1002/jnr.25000 (Epub ahead of print. PMID: 35043482).

Citrigno, L., Muglia, M., Qualtieri, A., Spadafora, P., Cavalcanti, F., Pioggia, G., et al., 2020. The mitochondrial dysfunction hypothesis in autism Spectrum disorders: current status and future perspectives. Int. J. Mol. Sci. 21 (16), 5785.

Dana, H., Tahtasakal, R., Sener, E.F., 2020a. Animal models of autism: a perspective from autophagy mechanisms. J Transl Genet Genom. 4, 251–262.

Dana, H., Bayramov, K.K., Delibasi, N., Tahtasakal, R., Bayramov, R., Hamurcu, Z., Sener, E.F., 2020b. Disregulation of autophagy in the transgenerational Cc2d1a mouse model of autism. NeuroMolecular Med. 22 (2), 239–249.

Del Pino, I., Rico, B., Marín, O., 2018. Neural circuit dysfunction in mouse models of neurodevelopmental disorders. Curr. Opin. Neurobiol. 48, 174–182.

Deng, Z., Zhou, X., Lu, J.H., Yue, Z., 2021. Autophagy deficiency in neurodevelopmental disorders. Cell Biosci. 11 (1), 214.

Forrest, M.P., Hill, M.J., Kavanagh, D.H., Tansey, K.E., Waite, A.J., Blake, D.J., 2018. The psychiatric risk gene transcription factor 4 (TCF4) regulates neurodevelopmental pathways associated with schizophrenia, autism, and intellectual disability. Schizophr. Bull. 44 (5), 1100–1110.

Golden, C.E., Buxbaum, J.D., De Rubeis, S., 2018. Disrupted circuits in mouse models of autism spectrum disorder and intellectual disability. Curr. Opin. Neurobiol. 48, 106–112.

Hamurcu, Z., Delibasi, N., Gecene, S., Sener, E.F., Donmez-Altuntas, H., Ozkul, Y., et al., 2018. Targeting LC3 and Beclin-1 autophagy genes suppresses proliferation, survival, migration and invasion by inhibition of Cyclin-D1 and uPAR/Integrin β1/ Src signaling in triple negative breast cancer cells. J. Cancer Res. Clin. Oncol. 144 (3), 415–430.

Heemers, H.V., Tindall, D.J., 2007. Androgen receptor (AR) coregulators: a diversity of functions converging on and regulating the AR transcriptional complex. Endocr. Rev. 28 (7), 778–808.

Hui, K., Katayama, Y., Nakayama, K.I., Nomura, J., Sakurai, T., 2020. Characterizing vulnerable brain areas and circuits in mouse models of autism: towards understanding pathogenesis and new therapeutic approaches. Neurosci. Biobehav. Rev. 110, 77–91.

Iossifov, I., O'Roak, B.J., Sanders, S.J., Ronemus, M., Krumm, N., Levy, D., Stessman, H. A., Witherspoon, K.T., et al., 2014. The contribution of de novo coding mutations to autism spectrum disorder. Nature. 515 (7526), 216–221.

Kim, J., Kundu, M., Viollet, B., Guan, K.L., 2011. AMPK and mTOR regulate autophagy through direct phosphorylation of Ulk1. Nat. Cell Biol. 13, 132–141.

Kim, H.J., Cho, M.H., Shim, W.H., Kim, J.K., Jeon, E.Y., Kim, D.H., Yoon, S.Y., 2017. Deficient autophagy in microglia impairs synaptic pruning and causes social behavioral defects. Mol. Psychiatry 22 (11), 1576–1584.

Lee, K.M., Hwang, S.K., Lee, J.A., 2013. Neuronal autophagy and neurodevelopmental disorders. Exp Neurobiol. 22, 133–142.

Lieberman, O.J., Cartocci, V., Pigulevskiy, I., Molinari, M., Carbonell, J., Broseta, M.B., et al., 2020. mTOR suppresses macroautophagy during striatal postnatal development and is hyperactive in mouse models of autism Spectrum disorders. Front. Cell. Neurosci. 14, 70.

Lombardo, M.V., Auyeung, B., Pramparo, T., Quartier, A., Courraud, J., Holt, R.J., Waldman, J., Ruigrok, A.N.V., Mooney, N., Bethlehem, R.A.I., Lai, M.C., Kundu, P., Bullmore, E.T., Mandel, J.L., Piton, A., Baron-Cohen, S., 2020. Sex-specific impact of prenatal androgens on social brain default mode subsystems. Mol. Psychiatry 25 (9), 2175–2188.

Mossa, A., Manzini, M.C., 2019. Molecular causes of sex-specific deficits in rodent models of neurodevelopmental disorders. J. Neurosci. Res. 99 (1), 37–56.

Nakamura, A., Naito, M., Tsuruo, T., Fujita, N., 2008. Freud-1/Aki1, a novel PDK1-interacting protein, functions as a scaffold to activate the PDK1/Akt pathway in epidermal growth factor signaling. Mol. Cell. Biol. 28, 5996–6009.

Oaks, A.W., Zamarbide, M., Tambunan, D.E., Santini, E., Di Costanzo, S., Pond, H.L., et al., 2017. Cc2d1a loss of function disrupts functional and morphological development in forebrain neurons leading to cognitive and social deficits. Cereb. Cortex 27, 1670–1685.

Ozkul, Y., Taheri, S., Bayram, K.K., Sener, E.F., Mehmetbeyoglu, E., Oztop, D.B., et al., 2020. A heritable profile of six miRNAs in autistic patients and mouse models. Sci. Rep. 10 (1), 9011.

Pourhamzeh, M., Moravej, F.G., Arabi, M., Shahriari, E., Mehrabi, S., Ward, R., et al., 2021. The roles of serotonin in neuropsychiatric disorders. Cell. Mol. Neurobiol. https://doi.org/10.1007/s10571-021-01064-9.

Sade, Y., Toker, L., Kara, N.Z., Einat, H., Rapoport, S., Moechars, D., et al., 2016. IP3 accumulation and/or inositol depletion: two downstream lithium's effects that may mediate its behavioral and cellular changes. Transl. Psychiatry 6 (12), e968.

Sener, E.F., Cıkılı Uytun, M., Korkmaz Bayramov, K., Zararsız, G., Oztop, D.B., Canatan, H., Ozkul, Y., 2016. The roles of CC2D1A and HTR1A gene expressions in autism spectrum disorders. Metab. Brain Dis. 31 (3), 613–619.

Sener, E.F., Onal, M.G., Dal, F., Nalbantoglu, U., Ozkul, Y., Canatan, H., Oztop, D.B., 2020. Novel alterations of *CC2D1A* as a candidate gene in a Turkish sample of patients with autism Spectrum disorder. Int J Neurosci. 7, 1–9.

Sener, E.F., Dana, H., Tahtasakal, R., Hamurcu, Z., Guler, A., Tutar, E., Doganyigit, Z., Rassoulzadegan, M., 2023. Partial changes in apoptotic pathways in hippocampus and hypothalamus of Cc2d1a heterozygous. Metab. Brain Dis. 38 (2), 531–541.

Sharma, A., Hoeffer, C.A., Takayasu, Y., Miyawaki, T., McBride, S.M., Klann, E., Zukin, R. S., 2010. Dysregulation of mTOR signaling in fragile X syndrome. J. Neurosci. 30, 694–702.

Tang, G., Gudsnuk, K., Kuo, S.H., Cotrina, M.L., Rosoklija, G., Sosunov, A., et al., 2014. Loss of mTOR-dependent macroautophagy causes autistic-like synaptic pruning deficits. Neuron. 83 (5), 1131–1143.

Wang, Y.C., Chen, C.H., Yang, C.Y., Ling, P., Hsu, K.S., 2023. High-fat diet exacerbates autistic-like restricted repetitive behaviors and social abnormalities in CC2D1A conditional knockout mice. Mol. Neurobiol. 60 (3), 1331–1352.

Werling, D.M., 2016. The role of sex-differential biology in risk for autism spectrum disorder. Biol. Sex Differ. 7, 58.

Wu, X., Li, W., Zheng, Y., 2020. Recent Progress on relevant microRNAs in autism Spectrum disorders. Int. J. Mol. Sci. 21 (16), E5904.

Yan, J., Porch, M.W., Court-Vazquez, B., Bennett, M.V.L., Zukin, R.S., 2018. Activation of autophagy rescues synaptic and cognitive defcits in fragile X mice. Proc. Natl. Acad. Sci. U. S. A. 115, E9707–E9716.

Yang, C.Y., Yu, T.H., Wen, W.L., Ling, P., Hsu, K.S., 2019. Conditional deletion of CC2D1A reduces hippocampal synaptic plasticity and impairs cognitive function through Rac1 Hyperactivation. J. Neurosci. 39 (25), 4959–4975.

Zamarbide, M., Mossa, A., Muñoz-Llancao, P., Wilkinson, M.K., Pond, H.L., Oaks, A.W., Manzini, M.C., 2019. Male-specific cAMP signaling in the Hippocampus controls spatial memory deficits in a mouse model of autism and intellectual disability. Biol. Psychiatry 85 (9), 760–768.

Zhang, J., Zhang, J.X., Zhang, Q.L., 2016. PI3K/AKT/mTOR-mediated autophagy in the development of autism spectrum disorder. Brain Res. Bull. 125, 152–158.

Zhang, Y., Li, N., Li, C., Zhang, Z., Teng, H., Wang, Y., Zhao, T., Shi, L., Zhang, K., Xia, K., Li, J., Sun, Z., 2020. Genetic evidence of gender difference in autism spectrum disorder supports the female-protective effect. Transl. Psychiatry 10 (1), 4.